energies

MDPI

Article

Advanced Universal Hybrid Power Filter Configuration for Enhanced Harmonic Mitigation in Industrial Power Systems: A Field-Test Approach

Mohsen Davoodi [1,*], Paul Hoevenaars [1], Hamed Jafari Kaleybar [2] and Morris Brenna [2]

[1] Mirus International Inc., Brampton, ON L6S 5P6, Canada; paul.hoevenaars@mirusinternational.com
[2] Energy Department, Politecnico di Milano, 20156 Milan, Italy; hamed.jafari@polimi.it (H.J.K.); morris.brenna@polimi.it (M.B.)
* Correspondence: mohsen.davoodi@mail.polimi.it or mason.davoodi@mirusinternational.com

Abstract

Power quality is a critical concern for large-scale industrial operations, necessitating advanced power conditioning equipment to maintain optimal performance and efficiency. Shunt active power filters (APFs) have gained significant attention for their profound impact on power quality, being valued for their system applicability, efficiency, and eco-friendliness. This study investigates the performance of an APF module connected upstream of a wide spectrum passive filter, the Advanced Universal Harmonic Filter (AUHF). The hybrid connection aims to reduce current total harmonic distortion (THDi) more effectively than using either the AUHF or the APF alone. Tests conducted under half-load and full-load conditions evaluate the performance of passive filters, active filters, and a hybrid configuration combining both. Results show that the hybrid configuration offers superior harmonic mitigation compared to individual filters. At full-load test, the combination of APF and AUHF reduced THDi to 1.2%, compared with 3.4% for the APF and 6.3% for the AUHF, demonstrating the enhanced performance of the hybrid setup. At half-load test, the THDi was reduced to 1.8%, compared with 7.2% for the APF and 8% for the AUHF, confirming the hybrid connection's superior performance over the AUHF alone. Practical experiments corroborate these findings, demonstrating that the hybrid filter configuration not only meets but exceeds even the most stringent industrial power quality requirements. To further validate the experimental results, each test case was also simulated using Mirus SOLV v6.6.4b12 software. Comprehensive data underscores the hybrid filter's potential as the optimal solution for significant power quality improvements. This research supports the adoption of hybrid filtering solutions, offering a reliable, efficient, and environmentally friendly approach to power quality management in industrial power systems.

Keywords: current harmonics; harmonic mitigation; hybrid power filter; industrial power systems; power electronics; power quality

Academic Editor: José Matas

Received: 19 December 2025
Revised: 23 January 2026
Accepted: 26 January 2026
Published: 29 January 2026

1. Introduction

The significance of detecting, monitoring, and classifying power quality in electrical systems has grown recently due to economic considerations, security concerns, and efficiency gains associated with the proliferation of smart grids.

One power quality concern, harmonic distortion, can significantly impact the performance of an electrical power system. The extensive use of nonlinear loads such as the power electronic converters present in adjustable speed drives, switch-mode computer power

supplies, and energy-saving lamps, as well as interface converters between renewable energy generators and the power grid, has led to a rise in harmonic and inter-harmonic emissions across a broad spectrum of frequencies [1]. Harmonics and inter-harmonics, whether at low or high frequencies, can cause various adverse effects including flicker, equipment malfunction or overheating, increased network losses, communication system interference, and errors in control systems and digital meters [2,3].

A traditional method for harmonic suppression and reactive power compensation is the use of passive tuned trap filters. As a mature technology, these filters provide a simple structure, low cost, and large capacity, but they also have some weaknesses [4–7]:

- The filtering performance is highly dependent upon the power system's impedance, as the impedance of the power transmission line affects current flow in each branch according to Kirchhoff's current law. Performance can be poor in large power systems with low source impedance—a 'stiff' source.
- Multiple tuned filtering branches are often required since each LC branch can only compensate for a specific frequency harmonic. Additionally, there is a risk of series or parallel resonance, which complicates the design process.
- Resonance can occur between the internal impedance of the power system and the tuned trap filter, leading to harmonic amplification.
- They cannot dynamically attenuate harmonics or compensate for reactive power.
- They have considerable weight and volume.

Paper [8] introduces a novel passive filter design that reduces harmonic distortions and enhances the reliability of load commutated inverter (LCI) drives. The design addresses detuning effects, resonance elimination, and harmonic loading of capacitors, making it practical for real industrial applications; however, it is super expensive.

Optimal placement and sizing of passive harmonic filters in unbalanced distribution systems using a nonlinear multi-objective optimization approach solved by a genetic algorithm is addressed by [9]. Although voltage harmonic distortion, filter costs, and voltage unbalances are considered, current total harmonic distortion is not tackled.

An optimization algorithm for designing single-tuned filters in industrial power systems to reduce harmonic distortion is presented by [10]. The algorithm, based on the forest growth model, enables both local and global searches for optimal solutions. It accounts for variations in filter components and system parameters. Even in the best-case scenario where standard limits are surpassed, their test, implemented with a linear load, does not accurately reflect real-world conditions.

Ref. [11] investigates various passive filter topologies, optimizing the L-RLC filter for minimal harmonic distortion, stable voltage, and reduced power losses. The optimal filter is manufactured, and field tested for noise and power performance, and evaluated alongside other filters.

These various tuned trap passive harmonic filters have their limitations; however, an effective form is the wide spectrum passive harmonic filter [12].

Alternatively, APFs can be used effectively to enhance power quality by eliminating harmonics, compensating reactive power, correcting the power factor, and addressing other power quality issues such as voltage sag, swell, and three-phase imbalance in some cases. Advantages of APF technology includes [13–15]:

- Fast dynamic response performance.
- Reduction of harmonic distortion while compensating for the reactive power dynamically without being significantly influenced by the grid's parameters (performance is mostly independent of the power distribution system properties).
- APFs are capable of suppressing both supply current harmonics and reactive currents.
- APFs can often avoid harmful resonances with the power distribution systems.

- Smaller volume and lighter weight.

On the other hand, a drawback of APFs is the requirement for fast switching of high currents within their power circuits. This can lead to high-frequency noise and supraharmonics, which can cause electromagnetic interference (EMI) in the power distribution systems.

The authors of [16] discussed the development of a dq-Proportional Resonant control strategy for shunt active power filters, aimed at eliminating distortions in source currents under various loading conditions. The switching signals for the inverter are generated using a hysteresis current control scheme. While the THDi mitigation appears significant, it is important to note that this is still just a laboratory prototype and far from replicating real-world conditions.

Ref. [17] introduced an optimal algorithm to improve the adaptation of parameter settings by gradually reducing the population size across generations. These studies function to minimize harmonic pollution in systems with nonlinear sources and loads. However, the effectiveness of the optimized active power filter parameters can be influenced by factors like grid disturbances, voltage fluctuations, and environmental conditions.

Ref. [18] discusses a type of active power filter that offers advantages like a low DC-link voltage, extended operational range, and the ability to simultaneously compensate for reactive power, harmonics, and unbalanced power. It presents a multi-quasi-proportional-resonant controller with gain scheduling for a thyristor-controlled LC-coupling HAPF, effectively reducing steady-state current tracking errors and output current ripple.

A technique introduced by [19] to monitor the AC capacitor voltage in a grid-connected APF without additional voltage sensors. This approach helps prevent AC capacitor burnout due to harmonic currents and inverter voltage, with a minor average discrepancy between measured and predicted voltages.

Study [20] compares D-STATCOM and APF based on voltage wave measurements, and the 3rd and 5th harmonics using three different capacitor banks. Results from MATLAB/Simulink simulations indicate that APF consistently outperforms D-STATCOM in all analyzed parameters. However, in the industry, the aim is to mitigate harmonics up to the 50th or even 100th order.

Ref. [21] explores using Plug-in Hybrid Electric Vehicles (PHEVs) in vehicle-to-grid (V2G) mode as a substitute for active filter capacitors to prevent harmonic distortion in HVDC lines, considering the state of charge of PHEV batteries. The primary goal of designing the controller is to manage the switching of the PHEV converters, enabling a parking lot of electric vehicles to function as a filter for harmonic elimination.

Network background harmonic distortion is considered by [22] when defining the APF's reference current. The APF reference current focuses solely on the customer's contributions to harmonic distortion at the point of common coupling (PCC). By distinguishing between harmonic currents caused by the customer and the network, the required APF power can be minimized. However, if the reference harmonic impedance used does not closely match the actual harmonic impedance, it leads to inadequate compensation or overcompensation of harmonics.

Research [23] presents an adaptive harmonic detection method tailored for photovoltaic-active power filter (PV-APF) systems. By incorporating a sliding integrator and utilizing an L2 norm-based step size iteration, the proposed method effectively balances convergence speed and steady-state accuracy.

The research [24] analyzes the energy-saving impact of implementing a parallel APF in an electric grid, considering both static and dynamic power losses of the APF. By using polynomial approximation of the energy characteristics of power switches, the study determines the APF's own power losses. It presents analytical relationships between additional power losses in network resistance and higher current harmonics, specifically

THD of the current. Accounting for the APF's own power losses, the overall energy-saving effect from grid current harmonic compensation is evaluated. The findings indicate that in some cases, particularly when network resistance is low, the use of APF can reduce network power efficiency. Additionally, the APF may introduce voltage distortion at the connection point, necessitating the use of extra passive or hybrid filters. Study [25] tackles power quality challenges in microgrids resulting from nonlinear loads and unbalanced grid voltages caused by single-phase distributed generation. It presents an advanced control structure for shunt active power filters (SAPFs) utilizing finite control set model predictive control (FCS-MPC). The proposed approach improves input current quality and minimizes current ripple via a computationally efficient cost function.

Table 1 provides a detailed comparison of the studies in the specified literature, leading to a clearer understanding of the existing research gaps.

Table 1. Comparative analysis of studies on harmonic mitigation techniques.

Ref.	Year	Key Benefit	Key Limitations
[8]	2021	Novel passive filter design for LCI drives. Addresses detuning, resonance elimination, and harmonic loading.	Very expensive.
[9]	2024	Optimal placement and sizing of passive filters. Nonlinear multi-objective optimization approach.	Does not tackle current total harmonic distortion.
[10]	2024	Forest growth model algorithm for filter design. Accounts for passive filter component and system parameter variations.	Best-case scenario does not accurately reflect real-world conditions.
[11]	2024	Optimizes L-RLC filter for minimal distortion and stable voltage. Field tested for performance.	Specific application may not be broadly applicable.
[16]	2021	dq-Proportional Resonant control for distortion elimination. Significant THDi mitigation.	Laboratory prototype only. Not representative of real-world conditions.
[17]	2017	Optimal algorithm for parameter adaptation. Gradually reduces population size.	Effectiveness is influenced by grid disturbances, voltage fluctuations, and environmental conditions.
[18]	2021	Low DC-link voltage. Extended operational range. Simultaneous compensation for reactive power, harmonics, and unbalanced power.	Complex multi-quasi-proportional-resonant controller.
[19]	2023	Monitors AC capacitor voltage without additional sensors. Prevents AC capacitor burnout.	Minor average discrepancy between measured and predicted voltages.
[20]	2024	APF outperforms D-STATCOM in various parameters. Effective MATLAB/Simulink simulation results.	Industry needs mitigation up to the 50th or 100th harmonic order.
[21]	2020	Uses PHEVs in V2G mode to prevent harmonic distortion. Manages switching of PHEV converters.	Dependent on the state of charge of PHEV batteries.
[22]	2021	Focuses on customer contributions to harmonic distortion. Minimizes required APF power.	Inadequate compensation if reference harmonic impedance does not match actual impedance.
[23]	2020	Balances convergence speed and steady-state accuracy. Sliding integrator and L2 norm-based step size iteration.	Specific to PV-APF systems.
[24]	2020	Analyzes energy-saving impact of parallel APF. Evaluates power losses and harmonic compensation.	May reduce network power efficiency. May introduce voltage distortion.

Table 1. *Cont.*

Ref.	Year	Key Benefit	Key Limitations
[25]	2020	Improved control structure for SAPFs. Reduces current ripple via efficient cost function.	Focused on nonlinear loads and unbalanced voltages in microgrids.
[26]	2022	Simulates impact of harmonics on electric train substation. Measures THD of voltage and current.	Only the 11th filter effective in maintaining THD within standard limits.
This Study	2025	Significant Harmonic Mitigation (1.2% THDi). Innovative Configuration. Real-Time Field Testing. High Precision in Measurements.	-

Although previous studies demonstrate the effectiveness of passive and active harmonic filters, their limitations, such as load-dependent performance, limited harmonic coverage, and testing mainly under laboratory conditions, pose challenges in industrial applications requiring very low THDi, such as semiconductor manufacturing, data centers, and precision manufacturing.

To address these gaps this study presents a comprehensive real-time field-test application setup designed to evaluate the effectiveness of power quality improvement configurations, specifically harmonic mitigation in power systems. The following outlines the contributions made to the work:

1. Performance Outcome: Successfully achieved current total harmonic distortion (THDi) of 1.2%, indicating significant effectiveness in harmonic mitigation across tested configurations.
2. Novel Configuration: Present a novel hybrid configuration of APF and AUHF, achieving such a low THDi in both description and practice.
3. Setup and Testing Conditions: Real-time hardware tests include active power filters, passive power filters, a variable frequency drive, an electric motor, and main and auxiliary current transformers performing under both half-load and full-load conditions to compare different configurations of power quality filters.
4. Measurement Precision: Utilized newly calibrated measurement devices for accurate data collection, ensuring reliable test results. This process was conducted in accordance with key industrial standards, including IEEE Std 519 [27], to guarantee compliance with established power quality and harmonic distortion benchmarks.
5. Comparative Analysis: Conducted comprehensive comparisons across different filter configurations—passive, active, and hybrid—to understand their performance under varying load conditions.

The remainder of this paper is structured as follows: Section 2 outlines the APF control system and its associated methods, along with the standards and certifications adhered to during testing. The test setup is detailed in Section 3, followed by the test results in Section 4. A comprehensive discussion is provided in Section 5. Finally, the concluding remarks are evaluated in Section 6.

2. Materials and Methods

The objective of APF control is to produce accurate gating signals for the switching transistors, derived from the estimated compensation reference signals. The effectiveness of an APF is highly influenced by the control technique employed [28]. As such, the selection and implementation of the control strategy are critical to ensuring optimal APF performance.

One of the most effective control methods for APFs is the linear control technique, which has been successfully implemented in the Mirus Advanced Active Power Filter (AAPF). In this section, we will provide a detailed discussion of this control approach and its application.

2.1. Linear Control Technique

The linear control of an active power filter is implemented using a negative-feedback system, as depicted in Figure 1. In this control framework, the compensation current if is continuously compared with its corresponding reference signal i_{ref}. This comparison is processed through an error amplifier, which generates a control signal proportional to the difference between the measured and reference values. The control signal is then input into a pulse width modulation (PWM) controller, where it is compared against a repetitive sawtooth waveform to produce the gating signals for the APF's switching transistors.

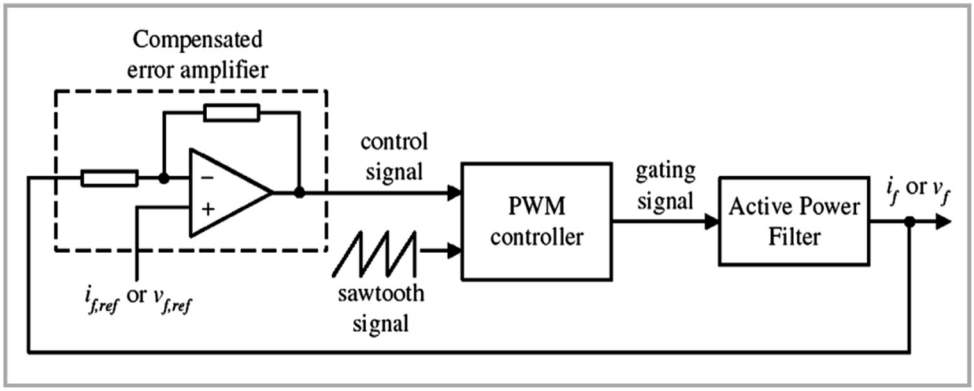

Figure 1. Linear control technique diagram [29].

The frequency of the sawtooth signal defines the switching frequency of the APF, which remains constant in linear control techniques. As illustrated in Figure 2, the gating signal is activated (set high) when the control signal exceeds the sawtooth waveform, and it is deactivated (set low) when the sawtooth signal surpasses the control signal. This process ensures precise control of the switching transistors, maintaining a stable and consistent compensation response. The constant switching frequency, a hallmark of linear control, provides reliable harmonic compensation and reduces the risk of instability in the filtering process.

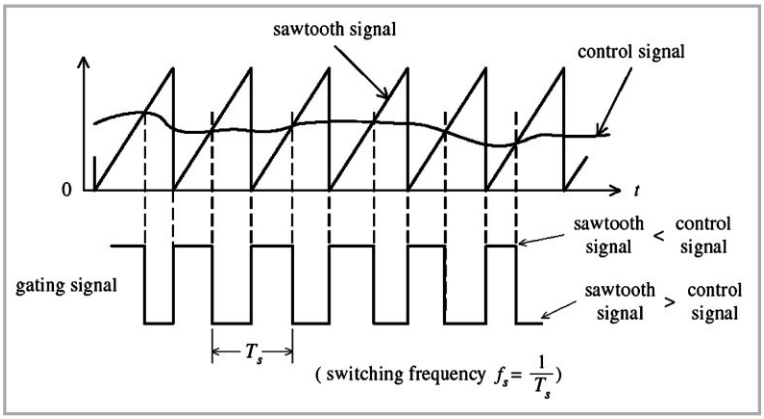

Figure 2. Gating signal generation by linear controller [29].

2.2. Signal Conditioning and Reference Current Generation

The control structure of the APF, as shown in Figure 3, involves continuous monitoring of both supply voltages and load currents. The three-phase grid voltages (u_{L1},u_{L2},u_{L3}) and load currents (i_{L1},i_{L2},i_{L3}) are sampled and transformed from the three-phase (abc) system to the d_q rotating reference frame using Park's transformation. Furthermore, the operating principles of the Mirus AAPF are presented in Figure 4.

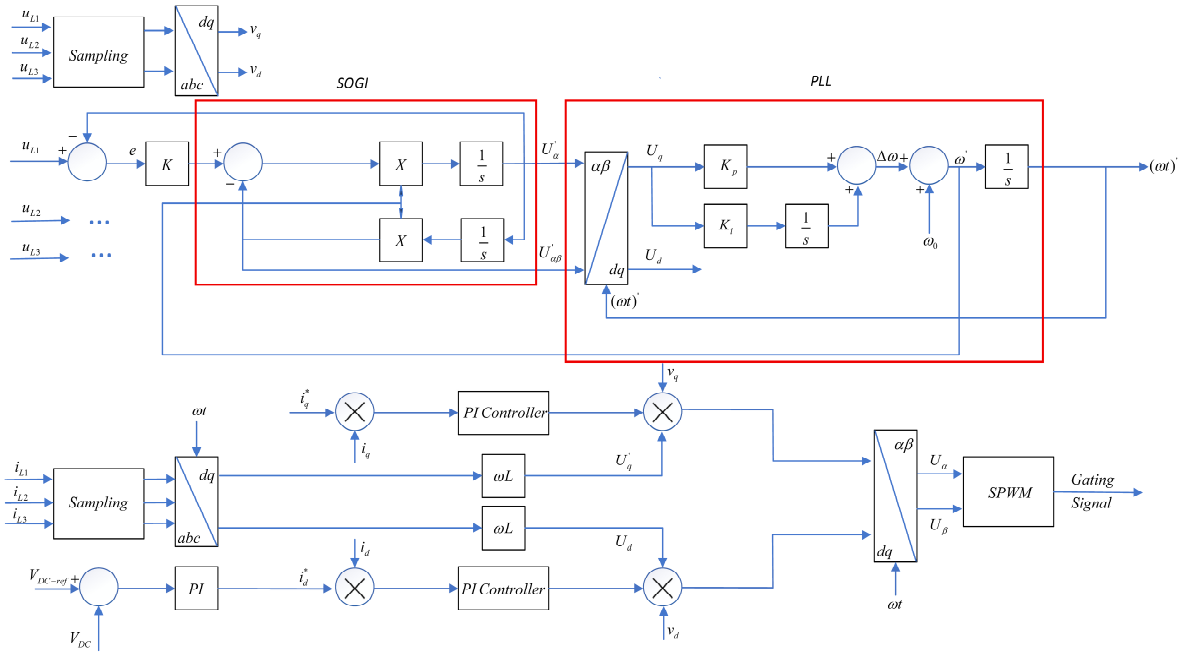

Figure 3. Block diagram of APF control system.

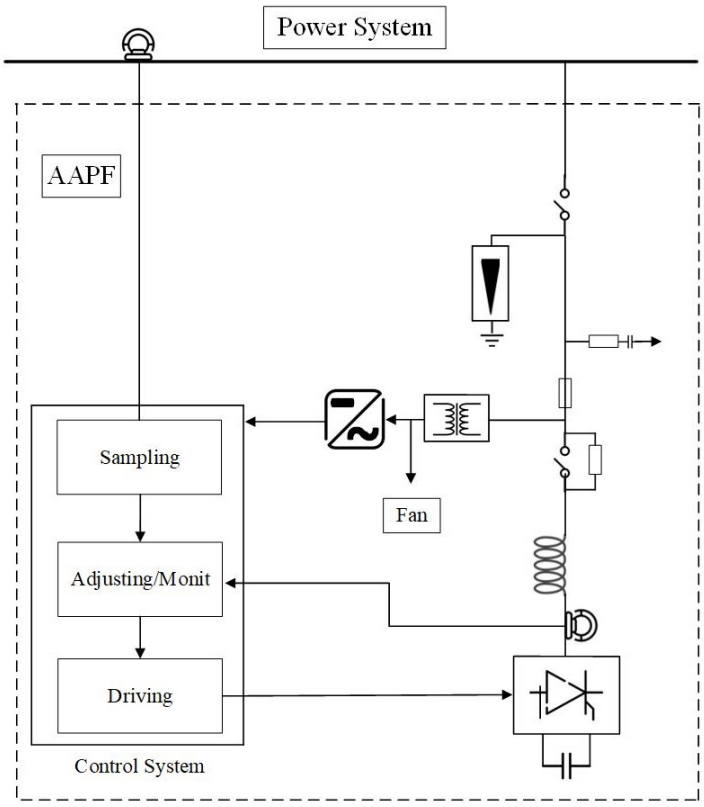

Figure 4. AAPF operation principles.

In the control of APF, the abc/d_q transformation, or Park's transformation, is a crucial technique for simplifying the control of three-phase AC systems. This method converts time-varying three-phase signals (abc) into two steady-state quantities in the synchronous rotating reference frame (d_q), allowing for more efficient regulation of active and reactive power components [30]. By decoupling the active (direct axis) and reactive (quadrature axis) components, the system achieves improved stability and performance in power quality applications.

Mathematically, the transformation from the stationary reference frame (abc) to the synchronous rotating reference frame (d_q) is expressed as follows [31]:

$$\begin{bmatrix} i_d \\ i_q \\ i_0 \end{bmatrix} = \frac{2}{3} \begin{pmatrix} \cos(\omega t) & \cos(\omega t - \frac{2\pi}{3}) & \cos(\omega t + \frac{2\pi}{3}) \\ -\sin(\omega t) & -\sin(\omega t - \frac{2\pi}{3}) & -\sin(\omega t + \frac{2\pi}{3}) \\ \frac{1}{2} & \frac{1}{2} & \frac{1}{2} \end{pmatrix} \begin{bmatrix} i_a \\ i_b \\ i_c \end{bmatrix} \quad (1)$$

where i_a, i_b, and i_c represent the instantaneous current values in the stationary abc frame, and i_d and i_q are the direct and quadrature components in the rotating d_q frame, respectively. Similarly, v_d, v_q denote phase voltages components in the d_q frame. The angular position of the reference frame, ωt, is synchronized with the grid voltage using a Phase-Locked Loop (PLL). This synchronization is essential for maintaining accurate alignment between the control system and the grid, which is critical for effective harmonic mitigation.

To further enhance the accuracy of the frequency estimation and ensuring accurate synchronization, particularly in the presence of distorted or unbalanced grid conditions, the Second-Order Generalized Integrator (SOGI) is employed in combination with the PLL. The SOGI provides a robust and precise estimation of the grid's fundamental frequency and phase angle, filtering out harmonic distortions and noise from the grid voltages [32]. This ensures that the extracted angular frequency ωt used in the d_q transformation is both accurate and responsive to dynamic grid conditions, improving the overall performance of the APF [33].

The reference currents (i_d^*, i_{q*}) are generated to meet the control objectives: i_d^* regulates the active current to control the DC bus voltage, while i_{q*} compensates for reactive power in the system. The DC bus voltage (Vdc) is compared to a reference value (V_{DCref}) with the error processed by a Proportional-Integral (PI) controller. This PI controller adjusts i_d^* to maintain the desired DC bus voltage, ensuring sufficient active power is drawn from the grid to stabilize the system. The reference currents are determined by the following equations, where P_{dc} is the DC component of active power:

$$\begin{bmatrix} i_\alpha \\ i_\beta \\ i_0 \end{bmatrix} = \frac{2}{3} \begin{pmatrix} cos(\omega t) & cos(\omega t - \frac{2\pi}{3}) & cos(\omega t + \frac{2\pi}{3}) \\ -sin(\omega t) & -sin(\omega t - \frac{2\pi}{3}) & -sin(\omega t + \frac{2\pi}{3}) \\ \frac{1}{2} & \frac{1}{2} & \frac{1}{2} \end{pmatrix} \begin{bmatrix} i_a \\ i_b \\ i_c \end{bmatrix} \quad (2)$$

$$\begin{bmatrix} v_\alpha \\ v_\beta \\ v_0 \end{bmatrix} = \frac{2}{3} \begin{pmatrix} cos(\omega t) & cos(\omega t - \frac{2\pi}{3}) & cos(\omega t + \frac{2\pi}{3}) \\ -sin(\omega t) & -sin(\omega t - \frac{2\pi}{3}) & -sin(\omega t + \frac{2\pi}{3}) \\ \frac{1}{2} & \frac{1}{2} & \frac{1}{2} \end{pmatrix} \begin{bmatrix} i_a \\ i_b \\ i_c \end{bmatrix} \quad (3)$$

$$\begin{bmatrix} p \\ q \end{bmatrix} = \begin{pmatrix} v_\alpha & v_\beta \\ -v_\beta & v_\alpha \end{pmatrix} \begin{bmatrix} i_\alpha \\ i_\beta \end{bmatrix} \quad (4)$$

$$\begin{bmatrix} i_{\alpha-ref} \\ i_{\beta-ref} \end{bmatrix} = -\frac{1}{{v^2}_\alpha + {v^2}_\beta} \begin{pmatrix} v_\alpha & -v_\beta \\ v_\beta & v_\alpha \end{pmatrix} \begin{bmatrix} p - p_{dc} \\ q \end{bmatrix} \quad (5)$$

The actual load currents (i_d,i_q) are then compared with the reference currents, and the resulting errors are processed by PI controllers to generate the control voltages u_d and u_q.

These voltages dictate the compensating current injected by the APF to closely track the reference signals, thus effectively mitigating harmonic distortion and compensating for reactive power.

The inverse transformation, which converts the dq quantities back to the abc frame, is given by:

$$\begin{bmatrix} i_a \\ i_b \\ i_c \end{bmatrix} = \begin{pmatrix} cos(\omega t) & sin(\omega t) & 1 \\ cos(\omega t - \frac{2\pi}{3}) & -sin(\omega t - \frac{2\pi}{3}) & 1 \\ cos(\omega t + \frac{2\pi}{3}) & -sin(\omega t + \frac{2\pi}{3}) & 1 \end{pmatrix} \begin{bmatrix} i_d \\ i_q \\ i_0 \end{bmatrix} \quad (6)$$

This inverse transformation is essential in generating appropriate gating signals for the APF's inverter, enabling the system to inject compensating currents back into the grid [32].

The control voltages u_d and u_q are transformed back into the stationary reference frame (abc) using the inverse Park transformation, resulting in voltages U_α and U_β. These voltages are fed into a Sinusoidal Pulse Width Modulation (SPWM) block, which generates the switching signals for the APF's inverter. SPWM ensures efficient and precise switching of the inverter's transistors, enabling accurate harmonic cancellation and power quality improvement.

2.3. Standards and Certifications

The integration of new technologies into interconnected power systems poses significant challenges for the power industry and the scientific community. To address these issues, researchers are developing new standards and validation methods for control, interoperability, reliability of distributed energy resources, modern power equipment, and applications related to power system stability, operation, control, and cybersecurity [34].

The Harmonics and Energy Nonlinear Load Testing Lab at Mirus International Inc. (Brampton, ON, Canada) utilizes several key standards to ensure the high accuracy and reliability of its tests. These standards and certifications include Institute of Electrical and Electronics Engineers (IEEE), Underwriters Laboratories (UL), Canadian Standards Association (CSA), American Bureau of Shipping (ABS), and International Organization for Standardization (ISO). By adhering to these rigorous guidelines, the lab guarantees precise and dependable results in the validation of harmonics and energy performance for nonlinear loads. This paper presents the test procedures and outcomes, demonstrating the superior accuracy and reliability achieved through compliance with these industry standards.

2.3.1. IEEE Standards for Power Quality Compliance

The IEEE 519 standard, known as IEEE Recommended Practice and Requirements for Harmonic Control in Electric Power Systems, provides guidelines for controlling harmonics in electrical power systems to ensure power quality. It specifies limits on harmonic distortions for both individual and THD levels, focusing on maintaining a high standard of power quality for both utilities and end-users. This standard is essential for designing and operating electrical systems that minimize the adverse effects of harmonics on equipment performance and longevity [27].

The IEEE 1159 standard [35], IEEE Recommended Practice for Monitoring Electric Power Quality, provides guidelines for the monitoring and interpretation of power quality in electrical systems. This standard covers the measurement and characterization of various power quality phenomena, including voltage sags, swells, interruptions, transients, waveform distortions, and frequency variations. IEEE Std 1159 aims to establish a common framework for identifying and analyzing power quality issues, thereby helping to improve the reliability and performance of electrical power systems [35].

The IEEE 1459 standard [36], IEEE Standard Definitions for the Measurement of Electric Power Quantities Under Sinusoidal, Non-sinusoidal, Balanced, or Unbalanced Conditions,

provides comprehensive definitions and methodologies for measuring electric power quantities. This standard addresses the complexities of power measurement in various operating conditions, including sinusoidal and non-sinusoidal waveforms, and balanced and unbalanced systems. By standardizing these measurements, IEEE Std 1459 ensures consistency and accuracy in the calculation and interpretation of power quantities, which is essential for the design, operation, and analysis of modern electrical power systems.

Standards typically specify recommended values for controlling harmonic distortion to maintain power quality. For voltage harmonics, most countries adhere to the limits set by the international standard IEEE Std 519. Current harmonic emission limits are often derived from these voltage harmonic standards and are contingent upon the scale of the installation being evaluated.

The American standard IEEE Std 519 sets the limits for voltage harmonics in Low Voltage (LV) networks at 8% THD, and 5% for current harmonics as shown in Table 2. The standards also define limits for individual voltage harmonics 5%, extending up to the 50th harmonic. These limits are established to ensure the quality of power by controlling the distortion caused by higher-order harmonics.

Table 2. Voltage distortion limits [37].

Bus Voltage	Individual Harmonic (%)	THD (%)
$V \leq 1.0$ kV	5.0	8.0
1 kV < $V \leq 69$ kV	3.0	5.0
69 kV < $V \leq 161$ kV	1.5	2.5
161 kV < V	1.0	1.5

2.3.2. UL Standard for Safety and Reliability

UL establishes comprehensive safety standards aimed at ensuring the safety, performance, and reliability of products and systems across various industries, including electrical appliances, electronics, and building materials. These standards are meticulously developed to address critical safety concerns and regulatory requirements. Compliance with UL standards signifies that a product has been rigorously tested and meets the established safety criteria [37]. The versions of UL standards are as Table 3:

Table 3. Standards related to safety and reliability of products and systems.

Standard	Subject
UL 508A [38]	Industrial Control Panels.
UL 1012 [39]	Power Units Other Than Class 2.
UL 1741 [40]	Inverters, Converters, Controllers, and Interconnection System Equipment for Use with Distributed Energy Resources.

2.3.3. CSA Standard for Canadian Regulatory Requirements

CSA Standards are specifications developed by the CSA Group; a leading standards organization based in Canada. These standards are integral to establishing benchmarks for safety, performance, and quality across diverse sectors, including electrical and electronic products, energy, healthcare, and construction. CSA Standards are pivotal in guiding regulatory compliance and setting industry best practices both in Canada and internationally. The different versions of CSA include industrial control equipment (CSA C22.2 No. 14 [41]), general use power supplies (CSA C22.2 No. 107.1 [42]), and industrial products for hazardous locations (CSA C22.2 No. 286 [43]). CSA ensures that products and services adhere to recognized safety and performance criteria, thereby safeguarding public safety and facilitating global trade [44].

2.3.4. ABS Standard for Shipboard Power Quality Equipment

An ABS Standard refers to a specification developed by the American Bureau of Shipping (ABS), a globally recognized organization dedicated to establishing standards for the design, construction, and operational maintenance of marine-related facilities, including ships and offshore structures. These standards are essential for ensuring the safety, reliability, and environmental compliance of marine vessels and offshore platforms. ABS Standards encompass various aspects such as structural integrity, machinery, electrical systems, and safety management, offering a comprehensive framework for the maritime industry to achieve and maintain high levels of performance and safety [45], which has three main categories as guidelines for marine equipment and installations (ABS rules for building and classing marine vessels), standards for monitoring systems on ships (ABS guide for classification and certification of condition monitoring systems), and standards for offshore platforms and structures (ABS rules for building and classing offshore units and structures).

2.3.5. ISO Compliance and Quality Standards

An ISO standard is a set of internationally recognized guidelines and requirements established by the International Organization for Standardization (ISO). ISO is an independent, non-governmental organization that develops and publishes standards to ensure the quality, safety, efficiency, and interoperability of products, services, and systems across various industries and sectors. These standards provide a common framework that facilitates international trade, enhances product quality, improves safety, and promotes innovation [46], and quality management systems (ISO 9001 [47]) are implemented in this work.

3. Test Setup

In the field of power quality (PQ), Software-in-the-Loop (SIL) testing serves as a fundamental step in the development of control systems. This method allows for the testing of control software in a simulated environment where hardware components are represented by software models, enabling early detection of software bugs and functional verification without the need for physical hardware. SIL testing offers advantages such as reduced development costs, ease of debugging, and the ability to test under various conditions. However, to achieve better accuracy in PQ studies, research can be extended with the adaptation of real-time Hardware-in-the-Loop (HIL) testing for large and complex power systems. HIL testing integrates actual hardware components with a real-time simulator, comprising digital simulators, testing hardware equipment, and their digital and analog signal interfaces [48]. This approach enhances test accuracy by closely imitating real-world conditions, allowing for the validation of hardware interfaces and the performance of the entire system under dynamic conditions.

Moving beyond HIL, field testing provides the most comprehensive validation by encompassing the entire system's workflow from start to finish with all actual hardware components in place, without relying on simulations. This method ensures that all integrated parts function together as intended in real-world scenarios, offering unparalleled accuracy and reliability in assessing the system's functionality, performance, and robustness. This work has employed a field-testing approach for the active and passive power filters, performed to the highest accuracy and standards, ensuring the final product meets all specifications and performs flawlessly in its intended application. The detailed methodology and results of the field test are explained in the following sections.

3.1. Test

To analyze the performance of electrical filters under varying load conditions, this work defines specific operational scenarios. When the connected load to the filter operates under conditions where the filter injects half of its rated current into the network, this is referred to as a half-load condition. Conversely, when the connected load operates under conditions where the filter injects its full rated current into the network, this is known as a full-load condition. These conditions provide a basis for evaluating the efficiency and effectiveness of the filter in different operational states.

In this series of tests, we investigate the performance of the APF, and the AUHF, which is a passive filter, and the APF module when connected upstream of an AUHF filter. This setup is applied to an electric motor operated through a variable frequency drive (VFD) under both half-load and full-load conditions. The investigation proceeds as follows:

1. APF Connection Only: Connect only the APF to the network and investigate its impact on the network under half-load and full-load conditions.
2. AUHF Connection Only: Connect only the AUHF to the network and investigate its impact on the network under half-load and full-load conditions.
3. Hybrid Connection: Connect the APF upstream of the AUHF filter and investigate the impact of this hybrid connection on the network under half-load and full-load conditions.

The results from these tests will provide insights into the efficiency and effectiveness of different filtering configurations, contributing to the optimization of harmonic mitigation strategies in electrical networks.

3.2. APF

The fundamental principle of an APF involves leveraging power electronics technologies to generate specific current components that neutralize the harmonic currents produced by nonlinear loads. In this context, a shunt APF is employed, recognized as the most significant and widely adopted configuration for active filtering applications. As depicted in Figure 5, the principal configuration of a Voltage Source Inverter (VSI)-based shunt APF comprises a DC bus capacitor (Cf), power electronic switches (F_s = 13 kHz), and interfacing inductors (Lf). The shunt APF functions as a current source, compensating for harmonic currents caused by nonlinear loads. Its operation relies on injecting a compensation current equal to the distorted current, thereby eliminating the original distortion [29].

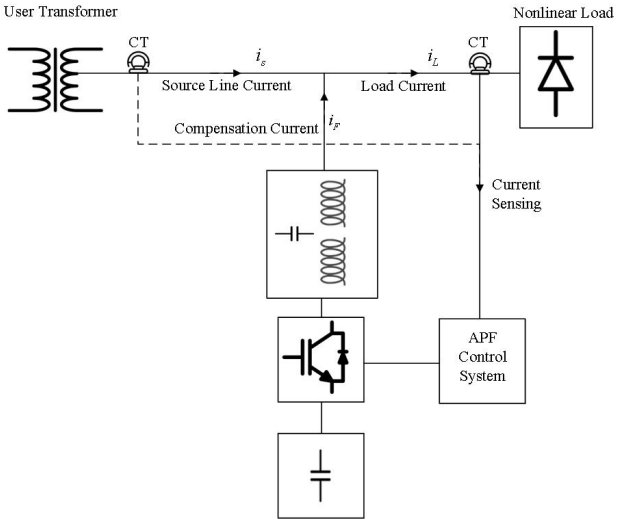

Figure 5. Principal configuration of a VSI-based shunt APF.

The nonlinear load current can be expressed as the sum of the fundamental current component ($i_{L,f}$) and the current harmonics ($i_{L,h}$) as follows:

$$i_l = i_{l,f} + i_{l,h} \tag{7}$$

The compensation current injected by the shunt APF should be:

$$i_f = i_{l,h} \tag{8}$$

The resultant source current is:

$$i_s = i_l - i_f = i_{l,f} \tag{9}$$

which exclusively comprises the fundamental component of the nonlinear load current, ensuring it is devoid of any harmonics, which are illustrated in Figure 6.

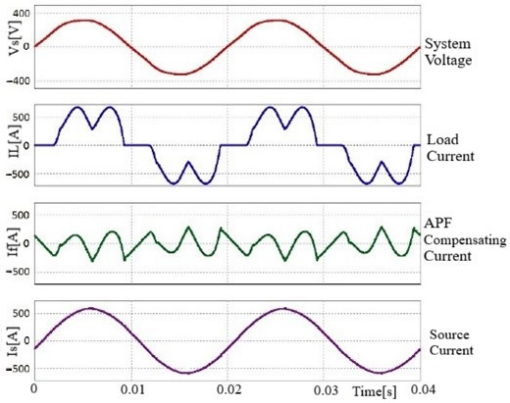

Figure 6. APF harmonic filtering operation principle [49].

The APF is designed to operate in parallel within the network architecture, as depicted in Figure 7. In this configuration, the system and the load are directly interconnected, with the APF connecting to each phase of both entities. Notably, in the context of a 3-wire system, a dedicated neutral connection is not depicted in the diagram. Additionally, the APF is appropriately linked to the protective earth, thereby ensuring comprehensive and secure electrical grounding throughout the circuit. This arrangement completes the electrical circuit and adheres to safety standards essential for reliable operation within the network environment.

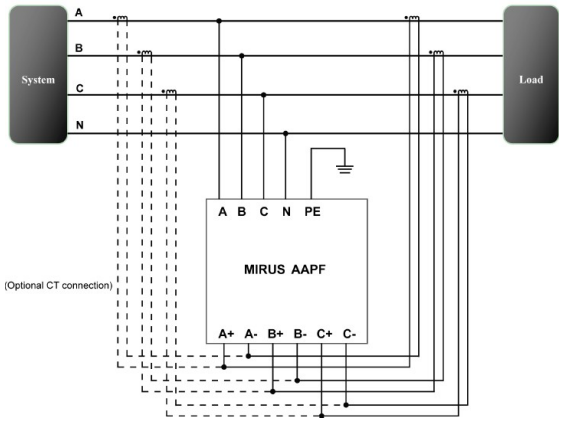

Figure 7. Equipment electrical wiring diagram [49].

Moreover, the primary current transformers (CTs) are strategically positioned on one side of either the APF system or the load. This positioning allows the CTs to accurately sense the current flow necessary for the control loop, facilitating effective operation and regulation within the network infrastructure.

3.3. PPF

The AUHF used in this work is a wide spectrum harmonic filter (WSHF) designed to attenuate a broad range of harmonic frequencies generated by nonlinear loads. WSHF is widely used due to its effectiveness in passive filtering applications. As illustrated in Figure 8, the primary configuration of a WSHF includes a network of capacitors (C_f) and inductors (L_f). This filter operates by providing low impedance paths for specific harmonic frequencies, thereby diverting these unwanted currents away from the main supply and mitigating harmonic distortion.

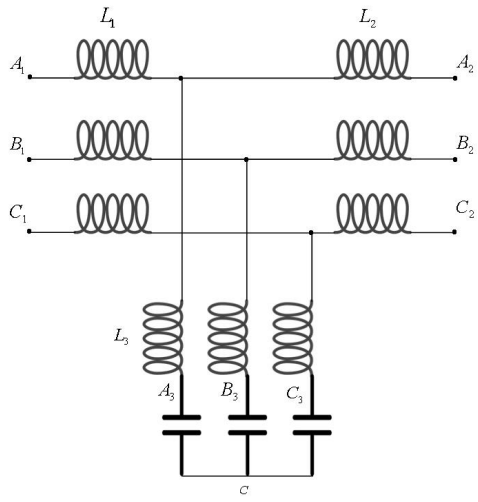

Figure 8. Lineator wide spectrum filter schematic.

Inductors (L_f) and capacitors (C_f) play crucial roles in blocking harmonics. Inductors present high impedance to high-frequency harmonic currents, thereby blocking them, while capacitors present low impedance to high-frequency harmonics, allowing these currents to bypass the main supply. This complementary behavior is leveraged to design effective harmonic filters.

The impedance (Z) of an inductor and a capacitor can be described by the following formulas:

$$Z_L = j\omega L \tag{10}$$

$$Z_C = \frac{1}{j\omega C} \tag{11}$$

where $\omega = 2\pi f$ is the angular frequency, f is the frequency, L is the inductance, and C is the capacitance.

At higher harmonic frequencies (higher f), the impedance of the inductor Z_L increases, effectively blocking these harmonics. Conversely, the impedance of the capacitor Z_C decreases at higher frequencies, providing a low impedance path for these harmonics to be shunted away from the main power supply.

The WSHF is designed to integrate seamlessly within various network architectures, as illustrated in Figure 9. In these configurations, the system and the loads are directly interconnected, with the WSHF connecting to each phase of the variable speed drive (VSD) systems. In standalone VSD systems, the WSHF is placed at the input to filter harmonics effectively before reaching the VSD/motor. In systems with a bypass, the WSHF

can remain connected to provide some compensation for the motor's reactive currents when the bypass is active. For multiple VSD systems, a single WSHF can service multiple drives, demonstrating its versatility and efficiency. This arrangement ensures that harmonic distortion is mitigated across all phases, promoting stable and reliable operation within the network environment while adhering to essential safety standards.

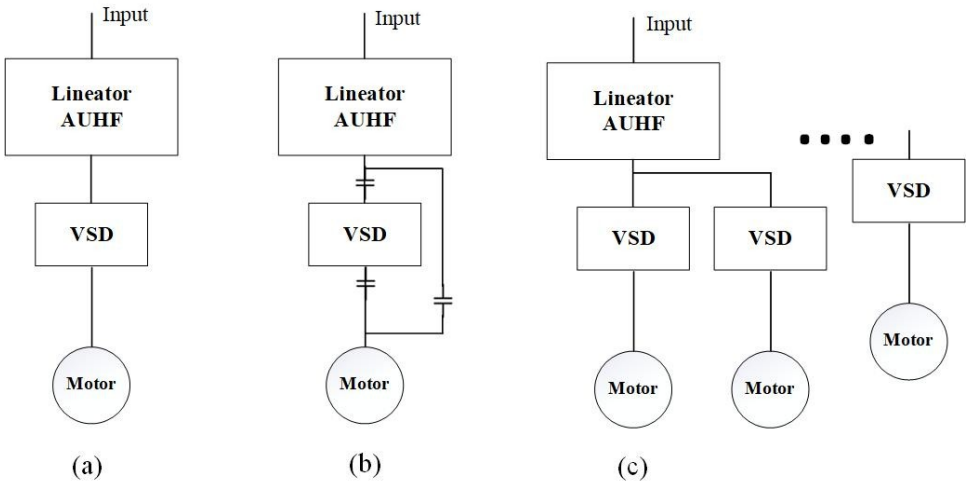

Figure 9. Typical lineator configurations. (**a**) Standalone VSD system. (**b**) VSD system with bypass. (**c**) Multiple VSD system.

3.4. Hybrid (APF + AUHF)

Historically, most controllers for APF were based on analog circuits, which are prone to signal drift. Digital controllers, using DSPs or microcontrollers, are preferred due to their flexibility and noise immunity. However, digital methods struggle with filtering high-order harmonics effectively because of the limitations in real-time sampling rates. Additionally, the use of fast-switching transistors like IGBTs in APFs introduces switching frequency noise, necessitating further filtering to avoid interference with sensitive equipment.

These technical limitations of conventional APFs can be addressed by hybrid APF configurations, which combine basic APFs with passive filters. Hybrid APFs leverage the advantages of both passive filters and APFs, offering enhanced performance and cost-effective solutions. The concept involves using a low-cost passive high-pass filter (HPF) alongside a conventional APF, the harmonic's filtering task is divided between the two filters: the APF cancels the lower order harmonics, while the AUHF filters the higher-order harmonics. The main objective of the hybrid APF is to improve the filtering performance of high-order harmonics while providing a cost-effective solution for mitigating low-order harmonics. Both the shunt APF and the passive filter are connected in parallel with the nonlinear load.

Various hybrid APFs have been reported in the literature, with two prominent configurations being the hybrid shunt APF and the hybrid series APF (Figure 10). The hybrid shunt APF connects both the shunt APF and passive filter in parallel with the nonlinear load, allowing the APF to cancel low-order harmonics and the HPF to filter higher-order harmonics. The hybrid series APF uses an interfacing transformer to couple the series APF to the distribution line, acting as a harmonic isolator and directing all nonlinear load current harmonics into the passive filter, effectively decoupling the source and load at undesired harmonic frequencies.

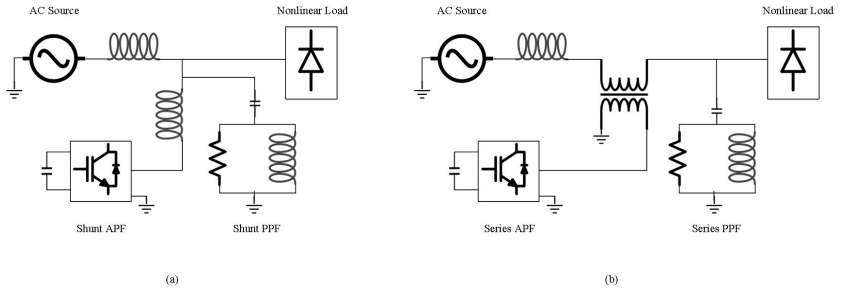

Figure 10. Hybrid APFs: (**a**) combination of shunt APF and shunt passive filter and (**b**) combination of series APF and series passive filter.

In this work, we utilize a novel hybrid configuration combining an APF with a WSHF, specifically the AUHF. The AUHF is directly connected to the AC input and subsequently to the motor through the VFD. The APF is positioned in parallel between the AC input and the AUHF. This configuration, illustrated in Figure 11, synergistically harnesses the strengths of both filters to achieve enhanced harmonic mitigation and overall system performance.

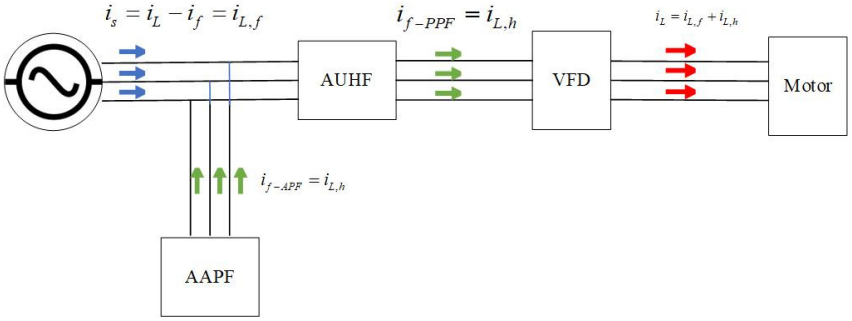

Figure 11. Hybrid configuration of APF and WSHF (AUHF).

The AUHF effectively mitigates most harmonics, while the APF addresses residual harmonics, significantly reducing THD and ensuring a disturbance-free waveform. This underscores the high quality and precision of both the designed APF and AUHF.

The wiring diagram for all test setups is 3P3W3 (3 Phase, 3 Wire, 3 Measurement) configuration as indicated in Figure 12. This setup ensures comprehensive and precise electrical connections essential for accurate measurement and analysis of power quality parameters. Each phase is individually wired with three conductors, facilitating effective monitoring and evaluation of harmonic distortion and reactive power compensation within the electrical network.

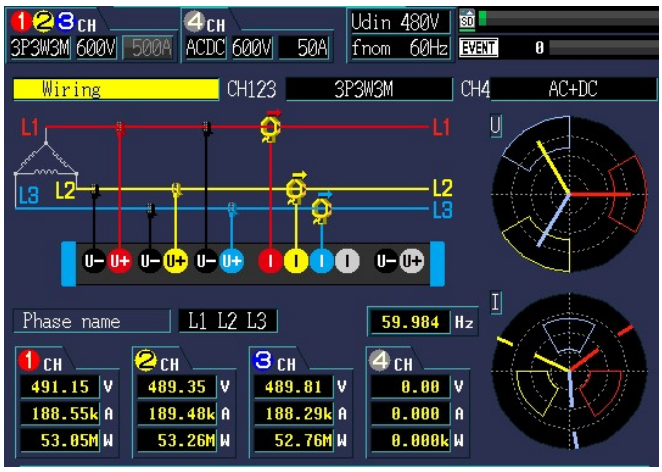

Figure 12. 3P3W3M wiring configuration for active/passive/hybrid power filter tests.

4. Tests and Results

To gain a comprehensive understanding of the performance of harmonic filters, this paper presents an analysis of six distinct scenarios, each featuring varying filter configurations and load levels, as depicted in Figure 13.

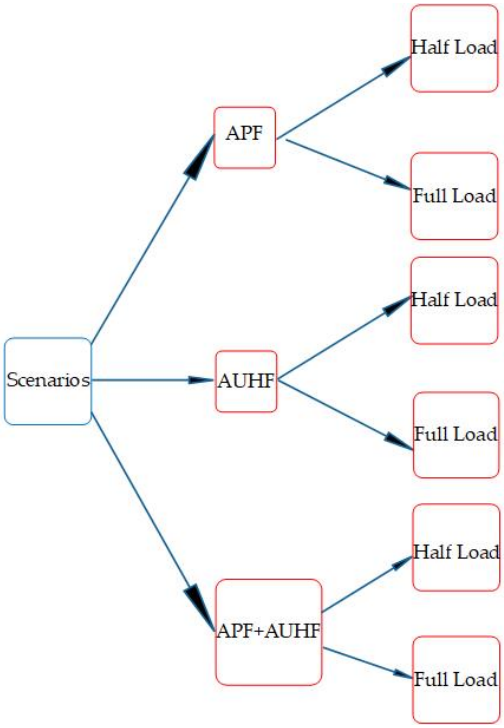

Figure 13. Scenario grid designed of harmonic filters, and load levels.

4.1. TEST1 (APF Half/Full Load)

This test was conducted to analyze the impact of active power filters on power quality within the power system. The procedure is as follows, with measurement devices and components detailed in Table 4.

Table 4. Test setup for APF half/full-load test.

R	Component	Specification
1	APF	Mirus International AAPF, 50 A, 480 V, Brampton, ON, Canada
2	APF's HMI	Mirus International, LCD touchscreen, Brampton, ON, Canada
3	APF Main CT, Side	Acrel, 800/5 A, Source Side, Shanghai, China
4	Measurement Device—Power Analyzer	Hioki (PQ3198), Ueda, Japan
5	Measurement Device—oscilloscope	Tektronix (DPO4014B), Beaverton, OR, USA
6	Measurement Device—Current Clamps	AEMC SR600 AC, 1000 A, Dover, DE, USA Hioki CT7136 (600 A)/9661, Ueda, Japan
7	Autotransformer	Mirus International, 600 V–480 V, Brampton, ON, Canada
8	VFD	Siemens 150 HP, Munich, Germany, Allen-Bradley 300 HP, Milwaukee, WI, USA
9	Cabling	Connection between VFD and Motors
10	M-G Set	Lincguard, 325 HP, Catharines, ON, Canada
11	Input Voltage (Line-to-Line)	480 VAC

To accurately monitor and analyze the electrical parameters at the source side, Hioki and Tektronix devices will be employed. This equipment will simultaneously measure three critical currents: the source current, the load current, and the current injected by the

active power filter. All equipment used in this process is in optimal condition, and the measurement devices have been meticulously calibrated to ensure the highest accuracy and quality.

The test procedure involved initially adjusting the VFD to operate at 60.23 Hz, resulting in the motor drawing 130 A. This adjustment caused the APF to inject half of its 50 A nominal current, operating under half-load conditions. Notably, despite the APF only injecting 25 A of harmonic current, it significantly mitigated harmonics, as evidenced by THDi of 7.2%. Furthermore, Figures 14 and 15 illustrate the three-phase current waveforms and the corresponding harmonic spectrum.

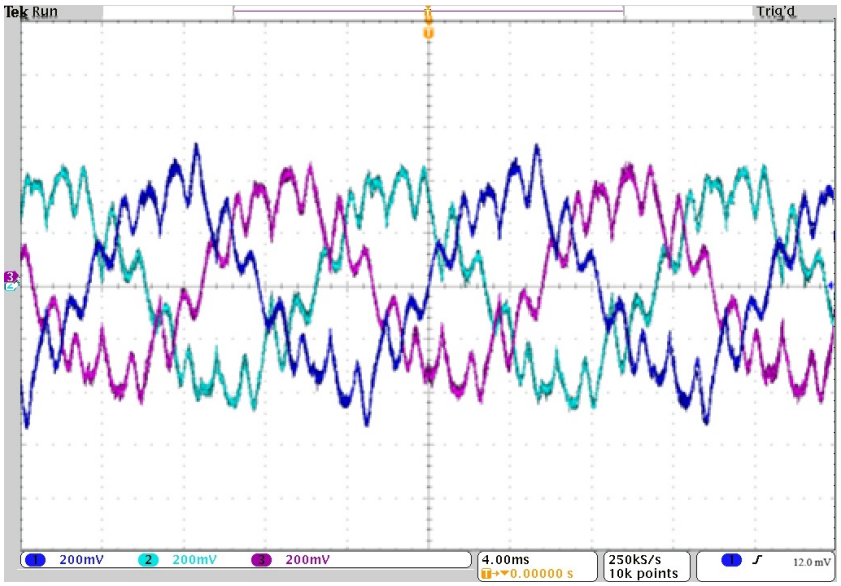

Figure 14. Three-phase source current waveform at half load of APF injected current.

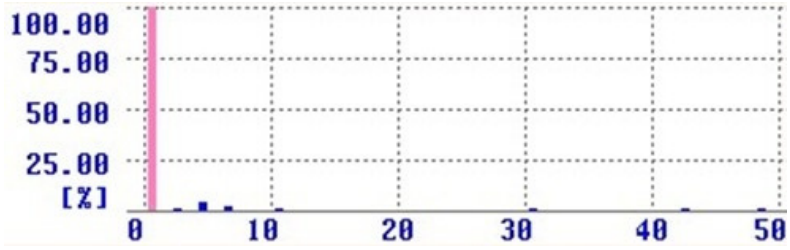

Figure 15. Three-phase current harmonics.

In the subsequent test phase, the VFD was adjusted to 60.45 Hz, causing the motor to draw 150 A, thereby prompting the APF to inject its entire nominal current into the power system, operating under full-load conditions. According to Table 5, this adjustment resulted in a significant reduction in THDi, achieving a notable 3.4%. This reduction represents a substantial improvement in harmonics mitigation for three-phase power systems.

Table 5. Test result for APF full-load test.

Rows	Element	Measurement
1	THDi (%)	3.4
2	Phase Voltage	277

Furthermore, Figures 16 and 17 depict the three-phase source current waveform under full load conditions and the corresponding harmonic spectrum. A comparison with the half-load condition reveals that the current waveforms exhibit markedly reduced distortion.

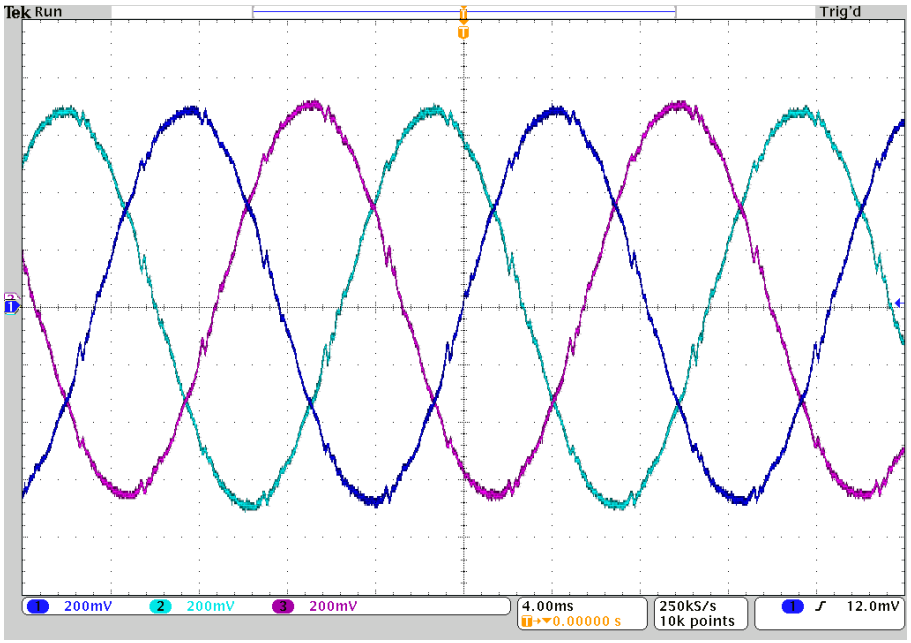

Figure 16. Three-phase source current waveform at full load of APF injected current.

Figure 17. Three-phase current harmonics.

4.2. TEST2 (AUHF Half/Full Load)

This evaluation aims to analyze the influence of AUHF, which is a passive harmonic filter on power quality within the electrical system. The procedure, along with the measurement devices and components, is detailed in Table 6.

Table 6. Test setup for AUHF half/full-load evaluation.

R	Component	Specification
1	AUHF	Mirus International AUHF, 450 HP, 480 V, Brampton, ON, Canada
2	Measurement Device-Power Analyzer	Hioki (PQ3198), Ueda, Japan
3	Measurement Device-oscilloscope	Tektronix (DPO4014B), Beaverton, OR, USA
4	Measurement Device—Current Clamps	AEMC SR600 AC, 1000 A, Dover, DE, USA, Hioki CT7136 (600 A)/9661, Ueda, Japan
5	Autotransformer	Mirus International, 600 V–480 V, Brampton, ON, Canada
6	VFD	Siemens 150 HP, Allen-Bradley 300 HP, Munich, Germany, Fuji Electric 200 HP, Tokyo, Japan
7	Cabling	Connection between VFD and Motors
8	M-G Set	Lincguard, 525 HP, Catharines, ON, Canada
9	Input Voltage (Line-to-Line)	480 VAC

Accurate monitoring and analysis of electrical parameters on the source side were carried out using Hioki and Tektronix instruments. These devices measured three key currents: source current, load current, and the current filtered by the AUHF. All equipment was in optimal condition, with calibration ensuring the highest precision.

The test began by setting the VFD to 60.23 Hz, resulting in the motor drawing 130 A. This setting caused the AUHF to operate at half load, filtering harmonic currents, and achieved a THDi of 8% as shown in Table 7. Figures 18 and 19 show the three-phase current waveforms and the harmonic spectrum.

Table 7. Test result for AUHF half-load test.

Rows	Element	Measurement
1	THDi (%)	8.0
2	Phase Voltage	277

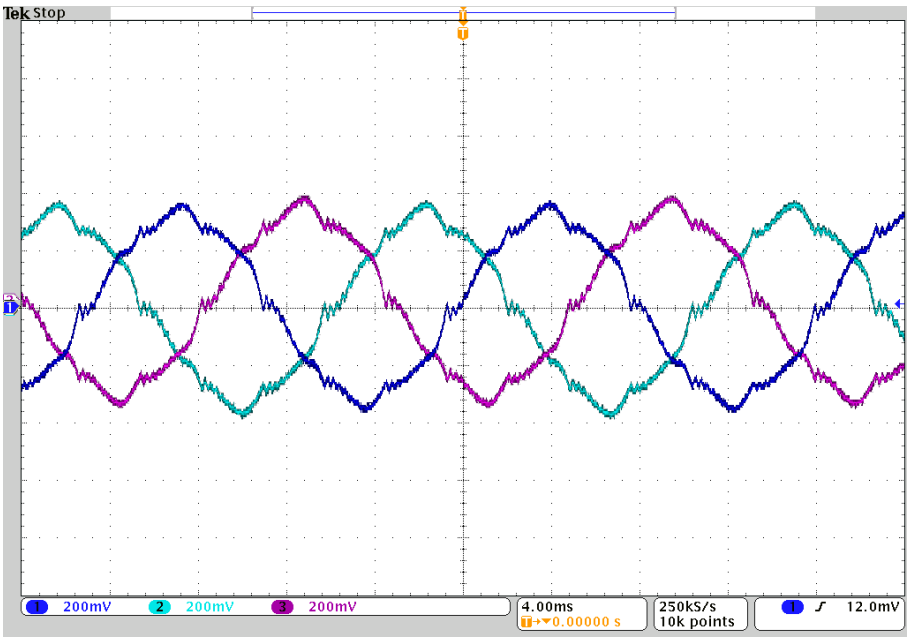

Figure 18. Three-phase source current waveform at half load of AUHF filtered current.

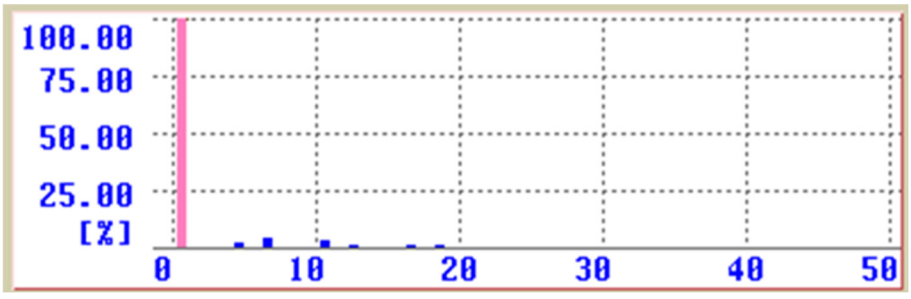

Figure 19. Three-phase current harmonics.

For the next phase, the VFD was set to 60.45 Hz, causing the motor to draw 150 A, prompting the AUHF to filter its full nominal current. This full-load condition significantly reduced THDi to 6.3% as shown in Table 8, marking a substantial improvement in harmonics mitigation for the three-phase power system.

Table 8. Test result for AUHF full-load test.

Rows	Element	Measurement
1	THDi (%)	6.3
2	Phase Voltage	277

Figures 20 and 21 present the three-phase source current waveform under full-load conditions and the corresponding harmonic spectrum. Compared to the half-load condition, the current waveforms show lightly reduced distortion.

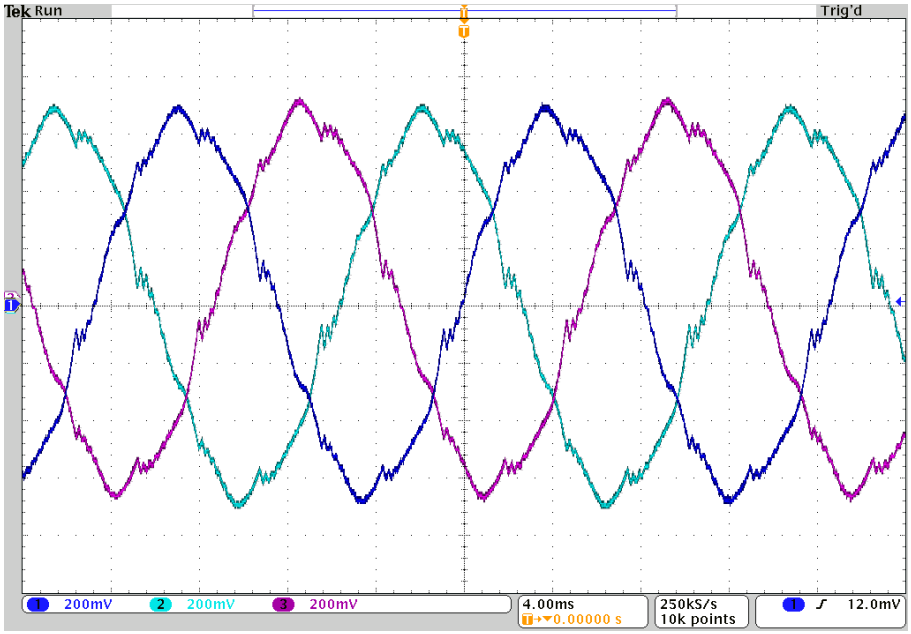

Figure 20. Three-phase source current waveform at full load of AUHF filtered current.

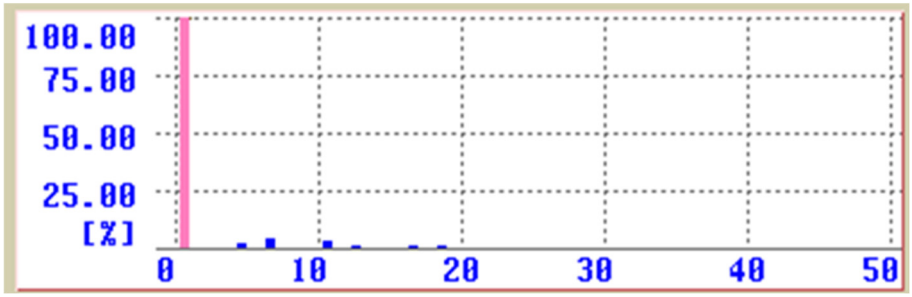

Figure 21. Three-phase current harmonics.

4.3. TEST3 (Hybrid Configuration: APF + AUHF Half/Full Load)

This final test in the sequence evaluates the combined impact of an APF and an AUHF on power quality within the electrical system. Table 9 details the test setup.

To ensure accurate monitoring and analysis of electrical parameters at the source side, Hioki and Tektronix instruments were utilized. These devices measured three critical currents: the source current, load current, and the current managed by the hybrid APF + AUHF system. All equipment was optimally maintained and precisely calibrated. Figure 22 depicts the laboratory test setup.

Table 9. Test setup for hybrid half/full-load evaluation.

R	Component	Specification
1	APF	Mirus International AAPF, 50 A, 480 V, Brampton, ON, Canada
2	APF's HMI	Mirus International, LCD touchscreen, Brampton, ON, Canada
3	AUHF	Mirus International AUHF, 450 HP, 480 V, Brampton, ON, Canada
4	APF main CT side	Acrel, 800/5 A, Source Side, Shanghai, China
5	Measurement Device-Power Analyzer	Hioki (PQ3198), Ueda, Japan
6	Measurement Device-oscilloscope	Tektronix (DPO4014B), Beaverton, OR, USA
7	Measurement Device—Current Clamps	AEMC SR600 AC, 1000 A, Dover, DE, USA Hioki CT7136 (600 A)/9661, Ueda, Japan
8	VFD	Allen-Bradley 300 HP, Fuji Electric 200 HP, Milwaukee, WI, USA
9	VFD	Siemens 150 HP, Munich, Germany
10	Autotransformer	Mirus International, 600 V–480 V, Brampton, ON, Canada
11	M-G Set	Lincguard, 525 HP, Catharines, ON, Canada
12	Cabling	Connection between VFD and Motors
13	Input Voltage (Line-to-Line)	480 VAC

Figure 22. Half/full-load test setup for hybrid APF + AUHF.

The test commenced by adjusting the VFD to operate at 60.23 Hz, resulting in the motor drawing 130 A. Under these conditions, the APF injected 25 A, while the AUHF provided complementary harmonic filtering. This hybrid configuration effectively reduced

harmonic distortions, achieving a total harmonic distortion of current (THDi) of 1.8% as shown in Table 10. Figures 23 and 24 illustrate the three-phase current waveforms and the harmonic spectrum, showing significantly fewer disturbances compared to conditions without the hybrid filter system.

Table 10. Test result for hybrid half-load test.

Rows	Element	Measurement
1	THDi (%)	1.8
2	Phase Voltage	277

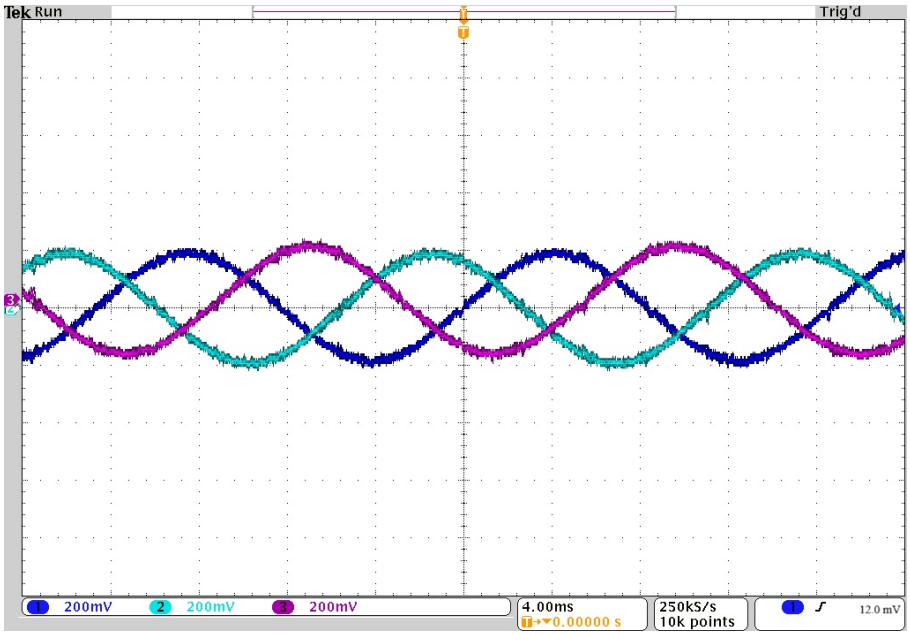

Figure 23. Three-phase source current waveform at half load with hybrid APF + AUHF.

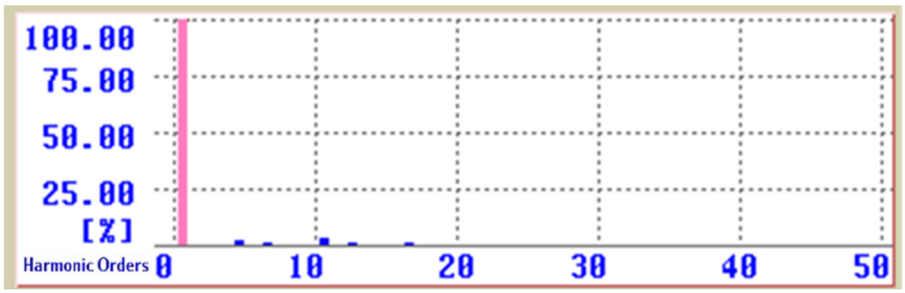

Figure 24. Three-phase current harmonics.

For the next phase, the VFD was adjusted to 60.45 Hz, causing the motor to draw 150 A. This led the APF to inject its full nominal current (50 A), while the AUHF continued to filter additional harmonics. Under full-load conditions, THDi was significantly reduced to 1.2% as shown in Table 11, demonstrating substantial improvement in harmonic mitigation for the three-phase power system.

Table 11. Test result for hybrid full-load test.

Rows	Element	Measurement
1	THDi (%)	1.2
2	Phase Voltage	277

Figures 25 and 26 present the three-phase source current waveform under full-load conditions and the corresponding harmonic spectrum. Compared to the half-load scenario, the current waveforms exhibited significantly reduced distortion, underscoring the effectiveness of the hybrid filter system. Also, three-phase power harmonics is illustrated in Figure 27 in vector presentation.

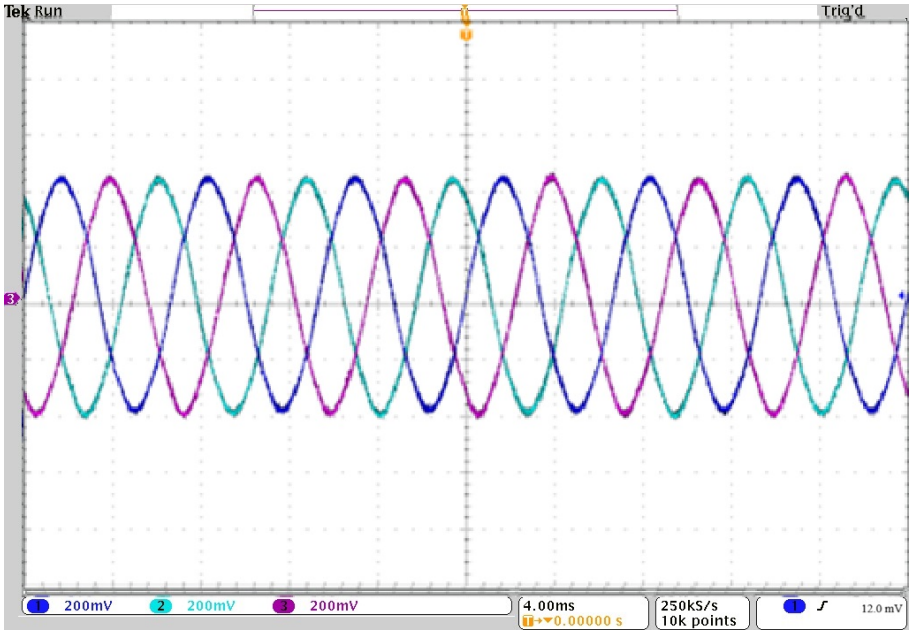

Figure 25. Three-phase source current waveform at full load with hybrid APF + AUHF.

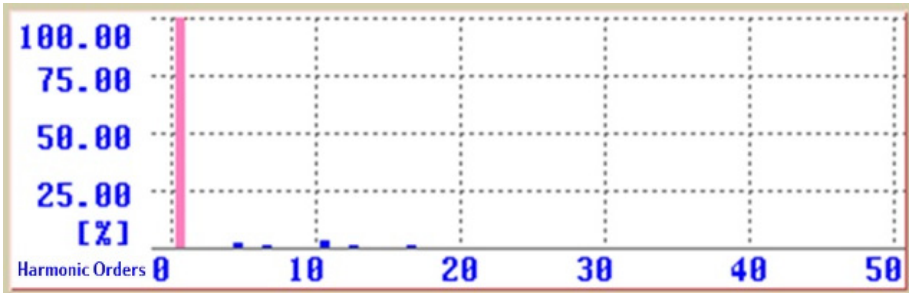

Figure 26. Three-phase current harmonics.

Figure 27. Three-phase power harmonics in vector presentation.

The purpose of this sequence of tests was to demonstrate the step-by-step improvement in harmonic mitigation and present a novel hybrid configuration of APF and PPF, achieving impressively low THD levels.

5. Discussion

5.1. Simulation Validation

To further substantiate the accuracy and reliability of our conducted tests, this paper simulated each test using Mirus SOLV v6.6.4b12 software as illustrated on Figures 28–30. The simulations precisely mirrored the experimental setups, replicating the exact conditions and configurations.

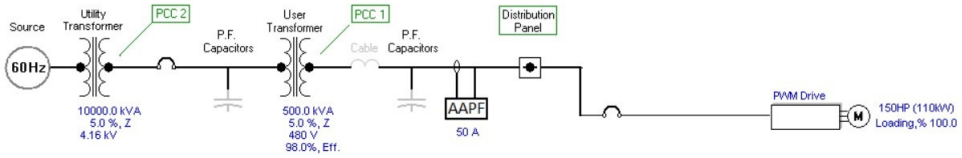

Figure 28. APF test setup simulation.

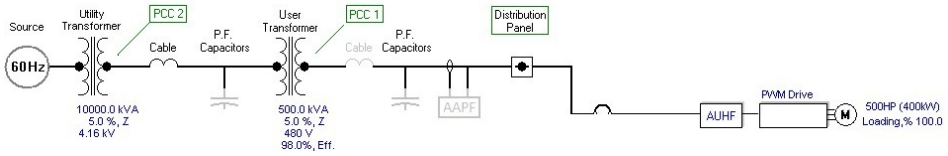

Figure 29. AUHF test setup simulation.

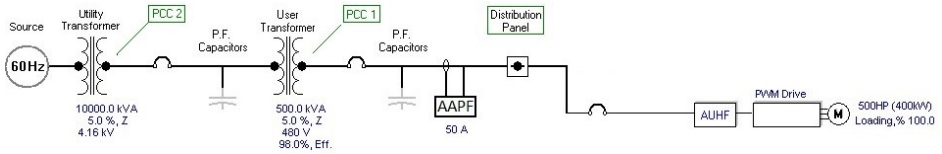

Figure 30. Hybrid configuration test setup simulation.

The resulting total harmonic distortion of current values from the simulations were compared with the experimental data. The simulations yielded THDi values and current waveforms that were in close alignment with the experimental results, demonstrating high accuracy and reliability of the APF (F_s = 13 kHz), AUHF, and their hybrid configuration. This congruence between simulated and experimental data underscores the effectiveness of the filters and the robustness of the test procedures. Figures 31–34 illustrate the simulation results for each test phase, showing minimal deviations from the experimentally obtained waveforms and THDi values.

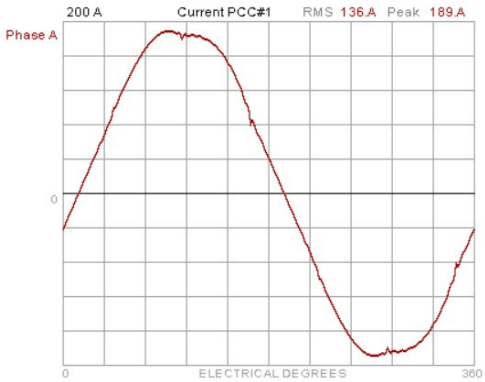

Figure 31. APF test result simulation. Phase source current waveform at full load of APF-injected current.

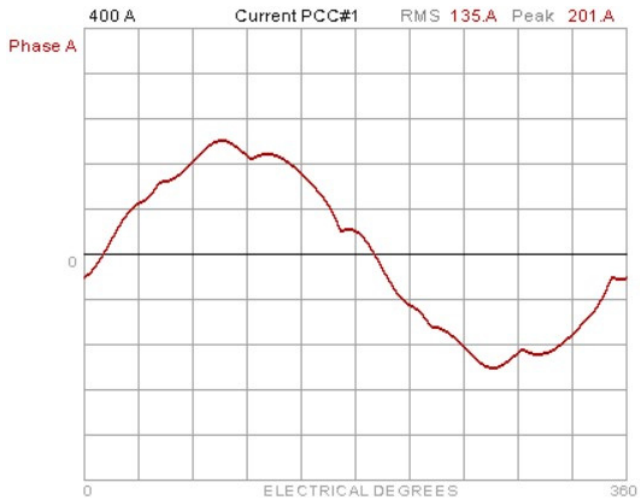

Figure 32. AUHF test result simulation. Phase source current waveform at full load of AUHF-injected current.

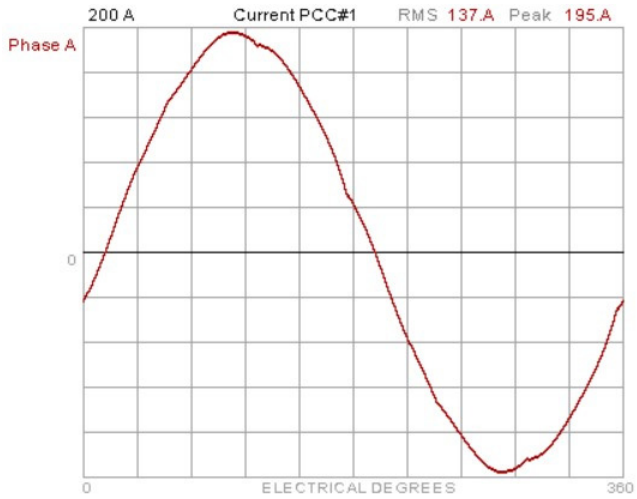

Figure 33. Hybrid configuration test result simulation. Phase source current waveform at full load current of Hybrid Conf.

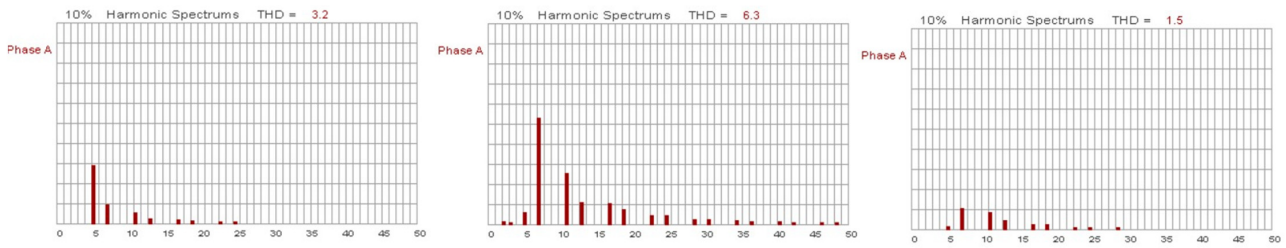

Figure 34. THDi measurement on common coupling point #1 for (**a**):APF, (**b**): AUHF, (**c**): hybrid configuration test setup.

5.2. Comparative Analysis

A comparative analysis of the three tests reveals a step-by-step improvement in harmonic mitigation, showcasing the effectiveness of the hybrid APF and PPF configuration. The following summary highlights the THDi improvements observed across the tests:

1. Test 1 (APF Half/Full Load):
   - Half Load: The variable frequency drive was set to 60.23 Hz, causing the motor to draw 130 A. The APF injected 25 A of harmonic current, reducing the THDi to 7.2%.
   - Full Load: With the VFD adjusted to 60.45 Hz, the motor drew 150 A, prompting the APF to inject its full nominal current of 50 A. This adjustment resulted in a THDi reduction to 3.4%.
2. Test 2 (AUHF Half/Full Load):
   - Half Load: The VFD was set to 60.23 Hz, causing the motor to draw 130 A. The AUHF operated at half load, filtering harmonic currents and achieving a THDi of 8.0%.
   - Full Load: With the VFD adjusted to 60.45 Hz, the motor drew 150 A, and the AUHF filtered its full nominal current. This resulted in a THDi reduction to 6.3%.
3. Test 3 (Hybrid Configuration: APF + AUHF Half/Full Load):
   - Half Load: The VFD was set to 60.23 Hz, causing the motor to draw 130 A. Under these conditions, the APF injected 25 A while the AUHF provided complementary harmonic filtering, achieving a THDi of 1.8%.
   - Full Load: With the VFD adjusted to 60.45 Hz, the motor drew 150 A. The APF injected its full nominal current of 50 A, while the AUHF continued to filter additional harmonics. This resulted in a THDi reduction to 1.2%.

These sequential tests clearly illustrate progressive improvements in THDi, with the hybrid configuration yielding the most significant reduction in harmonic distortion. The hybrid approach of combining APF and AUHF has demonstrated unprecedented effectiveness in mitigating harmonics, achieving the lowest THDi values recorded in both literature and practical applications.

These findings highlight the potential of the hybrid filter system to significantly enhance power quality in three-phase power systems, making it a promising solution for advanced harmonic mitigation. For better understanding, all test comparisons are summarized in Table 12.

Table 12. Comparative analysis table.

Test	Condition	VFD Frequency (Hz)	Voltage (V)	APF Current (A)	MOTOR Current (A)	AUHF Current (A)	THDi (%)
APF	Half Load	60.23	480	25	130	-	7.2
	Full Load	60.45	480	50	150	-	3.4
AUHF	Half Load	60.23	480	-	130	Half Load	8.0
	Full Load	60.45	480	-	150	Full Load	6.3
Hybrid	Half Load	60.23	480	25	130	Complementary	1.8
	Full Load	60.45	480	50	150	Complementary	1.2

6. Conclusions

This study demonstrates a systematic and substantial improvement in harmonic mitigation through a comparative analysis of three different configurations: active power filter (APF), Advanced Universal Harmonic Filter (AUHF), and a hybrid configuration combining both APF and AUHF. The results clearly indicate that the hybrid approach significantly outperforms individual filters in reducing total harmonic distortion (THDi) across various load conditions.

In Test 1, the APF alone showed a considerable reduction in THDi, achieving 7.2% at half load and 3.4% at full load. Test 2, which involved the AUHF, resulted in slightly higher

THDi values of 8.0% at half load and 6.3% at full load. However, Test 3, utilizing the hybrid configuration, marked a remarkable improvement, reducing THDi to 1.8% at half load and 1.2% at full load.

These findings underscore the hybrid configuration's effectiveness, achieving unprecedented THDi reduction levels. The hybrid system's superior performance is attributed to the complementary operation of APF and AUHF, which provide enhanced harmonic filtering capabilities.

Given the critical importance of power quality in large-scale industrial operations, the results of this study advocate for the adoption of hybrid filtering solutions. The hybrid APF and AUHF configuration not only meets but exceeds stringent industrial power quality standards, offering a reliable, efficient, and environmentally friendly approach to power quality management. This research highlights the potential of hybrid filters to deliver significant improvements in power quality, making them a compelling choice for modern industrial power systems.

Author Contributions: Conceptualization, M.B.; methodology, H.J.K.; software, P.H.; validation, M.D.; formal analysis, M.B.; investigation, P.H.; resources, P.H.; data curation, M.D.; writing—original draft preparation, M.D.; writing—review and editing, H.J.K.; visualization, H.J.K.; supervision, M.B.; project administration, P.H.; funding acquisition, P.H. All authors have read and agreed to the published version of the manuscript.

Funding: The authors declare that this study received funding from Paul Hoevenaars, General Manager at Mirus International Inc. The funder had the following involvement with the study: funding acquisition, project administration, resources, investigation, and software.

Data Availability Statement: The data presented in this study are available on request from the corresponding author.

Conflicts of Interest: Authors Mohsen Davoodi and Paul Hoevenaars were employed by Mirus International Inc. The remaining authors declare that the research was conducted in the absence of any commercial or financial relationships that could be construed as a potential conflict of interest. The authors declare that this study received funding from Paul Hoevenaars, General Manager at Mirus International Inc. The funder had the following involvement with the study: funding acquisition, project administration, resources, investigation, and software.

References

1. Arranz-Gimon, A.; Zorita-Lamadrid, A.; Morinigo-Sotelo, D.; Duque-Perez, O. A review of total harmonic distortion factors for the measurement of harmonic and interharmonic pollution in modern power systems. *Energies* **2021**, *14*, 6467. [CrossRef]
2. Kalair, A.; Abas, N.; Kalair, A.R.; Saleem, Z.; Khan, N. Review of harmonic analysis, modeling and mitigation techniques. *Renew. Sustain. Energy Rev.* **2017**, *78*, 1152–1187. [CrossRef]
3. Otcenasova, A.; Bolf, A.; Altus, J.; Regula, M. The influence of power quality indices on active power losses in a local distribution grid. *Energies* **2019**, *12*, 1389. [CrossRef]
4. Zhai, H.; Zhuo, F.; Zhu, C.; Yi, H.; Wang, Z.; Tao, R.; Wei, T. An optimal compensation method of shunt active power filters for system-wide voltage quality improvement. *IEEE Trans. Ind. Electron.* **2019**, *67*, 1270–1281.
5. Beres, R.N.; Wang, X.; Liserre, M.; Blaabjerg, F.; Bak, C.L. A review of passive power filters for three-phase grid-connected voltage-source converters. *IEEE J. Emerg. Sel. Top. Power Electron.* **2015**, *4*, 54–69.
6. da Silva, S.A.; Negrão, F.A. Single-phase to three-phase unified power quality conditioner applied in single-wire earth return electric power distribution grids. *IEEE Trans. Power Electron.* **2017**, *33*, 3950–3960. [CrossRef]
7. Motta, L.; Faúndes, N. Active/passive harmonic filters: Applications, challenges & trends. In Proceedings of the 2016 17th International Conference on Harmonics and Quality of Power (ICHQP), Belo Horizonte, Brazil, 16 October 2016; IEEE: New York, NY, USA, 2016; pp. 657–662.
8. Shakeri, S.; Esmaeili, S.; Koochi, M.H. Passive harmonic filter design considering voltage sag performance-applicable to large industries. *IEEE Trans. Power Deliv.* **2021**, *37*, 1714–1722. [CrossRef]

9. Milovanovic, M.J.; Raicevic, S.S.; Klimenta, D.O.; Raicevic, N.B.; Perovic, B.D. Determination of optimal locations and parameters of passive harmonic filters in unbalanced systems using the multiobjective genetic algorithm. *Elektronika ir Elektrotechnika* **2024**, *30*, 28–37. [CrossRef]
10. Lin, S.M.; Chou, C.J.; Lu, C.T.; Hsiao, Y.T. Optimal design of single-tuned filters for industrial power systems to reduce harmonic distortion using forest algorithm. *J. Chin. Inst. Eng.* **2024**, *47*, 414–422. [CrossRef]
11. Latoufis, K.C.; Vassilakis, A.I.; Grapsas, I.K.; Hatziargyriou, N.D. Design Optimization and Performance Evaluation of Passive Filters for Acoustic Noise Mitigation in Locally Manufactured Small Wind Turbines. *IEEE Trans. Ind. Appl.* **2024**, *60*, 4350–4365. [CrossRef]
12. Mirus International Inc. Available online: https://www.mirusinternational.com/downloads/MIRUS-WP003-A-Practical-and-Effective-Way-of-Applying-IEEEStd519-Harmonic-Limits.pdf (accessed on 11 January 2026).
13. Melo, I.D.; Pereira, J.L.; Variz, A.M.; Ribeiro, P.F. Allocation and sizing of single tuned passive filters in three-phase distribution systems for power quality improvement. *Electr. Power Syst. Res.* **2020**, *180*, 106128. [CrossRef]
14. Kaleybar, H.J.; Davoodi, M.; Brenna, M.; Zaninelli, D. Applications of genetic algorithm and its variants in rail vehicle systems: A bibliometric analysis and comprehensive review. *IEEE Access* **2023**, *11*, 68972–68993. [CrossRef]
15. Adak, S. Harmonics mitigation of stand-alone photovoltaic system using LC passive filter. *J. Electr. Eng. Technol.* **2021**, *16*, 2389–2396. [CrossRef]
16. Puhan, P.S.; Ray, P.K.; Pottapinjara, S. Performance analysis of shunt active filter for harmonic compensation under various non-linear loads. *Int. J. Emerg. Electr. Power Syst.* **2021**, *22*, 21–29.
17. Biswas, P.P.; Suganthan, P.N.; Amaratunga, G.A. Minimizing harmonic distortion in power system with optimal design of hybrid active power filter using differential evolution. *Appl. Soft Comput.* **2017**, *61*, 486–496. [CrossRef]
18. Sou, W.K.; Chao, C.W.; Gong, C.; Lam, C.S.; Wong, C.K. Analysis, design, and implementation of multi-quasi-proportional-resonant controller for thyristor-controlled LC-coupling hybrid active power filter (TCLC-HAPF). *IEEE Trans. Ind. Electron.* **2021**, *69*, 29–40. [CrossRef]
19. Lee, H.; Shon, J. Sensorless AC capacitor voltage monitoring method for HAPF. *IEEE Access* **2023**, *11*, 15514–15524. [CrossRef]
20. Taya, B.B.; Ahammad, A.; Jahin, F.I. Total harmonic distortion mitigation and voltage control using distribution static synchronous compensator and hybrid active power filter. *Int. J. Adv. Technol. Eng. Explor.* **2024**, *11*, 624. [CrossRef]
21. Fazaeli, M.H.; Keramat, M.M.; Alipour, H.; Khodabakhsi-javinani, N. Effects of Electric Vehicles Battery on The Harmonic Distortion of HVDC Lines by Active Filter. In Proceedings of the 2020 15th International Conference on Protection and Automation of Power Systems (IPAPS), Shiraz, Iran, 30 December 2020; IEEE: New York, NY, USA, 2020; pp. 93–98.
22. Špelko, A.; Blažič, B.; Papič, I.; Herman, L. Active filter reference calculations based on customers' current harmonic emissions. *Energies* **2021**, *14*, 220. [CrossRef]
23. Li, Z.; Wang, L.; Wang, Y.; Li, G. Harmonic detection method based on adaptive noise cancellation and its application in photovoltaic-active power filter system. *Electr. Power Syst. Res.* **2020**, *184*, 106308. [CrossRef]
24. Plakhtii, O.; Nerubatskyi, V.; Scherbak, Y.; Mashura, A.; Khomenko, I. Energy efficiency criterion of power active filter in a three-phase network. In Proceedings of the 2020 IEEE KhPI Week on Advanced Technology (KhPIWeek), Kharkiv, Ukraine, 5 October 2020; IEEE: New York, NY, USA, 2020; pp. 165–170.
25. Alhasheem, M.; Mattavelli, P.; Davari, P. Harmonics mitigation and non-ideal voltage compensation utilising active power filter based on predictive current control. *IET Power Electron.* **2020**, *13*, 2782–2793.
26. Kritsanasuwan, K.; Leeton, U.; Kulworawanichpong, T. Harmonic mitigation of AC electric railway power feeding system by using single-tuned passive filters. *Energy Rep.* **2022**, *8*, 1116–1124. [CrossRef]
27. *IEEE Std 519*; IEEE Recommended Practice and Requirements for Harmonic Control in Electric Power Systems. IEEE Standards Association: New York, NY, USA, 2014.
28. Buso, S.; Malesani, L.; Mattavelli, P.; Veronese, R. Design and fully digital control of parallel active filters for thyristor rectifiers to comply with IEC-1000-3-2 standards. *IEEE Trans. Ind. Appl.* **2002**, *34*, 508–517. [CrossRef]
29. Salam, Z.; Cheng, T.P.; Jusoh, A. *Review of Active Power Filter Technologies*; The Institution of Engineers: Petaling Jaya, Malaysia, 2007; Volume 68.
30. Saadat, H. *Power System Analysis*; McGraw-hill: New York, NY, USA, 1999.
31. Mohan, N.; Undeland, T.M.; Robbins, W.P. *Power Electronics: Converters, Applications, and Design*; John Wiley & Sons: Hoboken, NJ, USA, 2003.
32. Kaleybar, H.J.; Kojabadi, H.M.; Foiadelli, F.; Brenna, M.; Blaabjerg, F. Model analysis and real-time implementation of model predictive control for railway power flow controller. *Int. J. Electr. Power Energy Syst.* **2019**, *109*, 290–306. [CrossRef]
33. Singh, B.; Chandra, A.; Al-Haddad, K. *Power Quality: Problems and Mitigation Techniques*; John Wiley & Sons: Hoboken, NJ, USA, 2015.

34. Montoya, J.; Brandl, R.; Vishwanath, K.; Johnson, J.; Darbali-Zamora, R.; Summers, A.; Hashimoto, J.; Kikusato, H.; Ustun, T.S.; Ninad, N.; et al. Advanced laboratory testing methods using real-time simulation and hardware-in-the-loop techniques: A survey of smart grid international research facility network activities. *Energies* **2020**, *13*, 3267. [CrossRef]
35. *IEEE Std 1159*; IEEE Recommended Practice for Monitoring Electric Power Quality. IEEE Standards Association: New York, NY, USA, 2019.
36. *IEEE Std 1459*; IEEE Standard Definitions for the Measurement of Electric Power Quantities under Sinusoidal, Nonsinusoidal, Balanced, or Unbalanced Conditions. IEEE Standards Association: New York, NY, USA, 2010.
37. Underwriters Laboratories. Available online: https://www.shopulstandards.com/ProductDetail.aspx?UniqueKey=47339 (accessed on 11 January 2026).
38. *UL 508A*; Standard for Industrial Control Panels. Underwriters Laboratories: Northbrook, IL, USA, 2018.
39. *UL 1012*; Standard for Power Units Other than Class 2. Underwriters Laboratories: Northbrook, IL, USA, 2018.
40. *UL 1741*; Standard for Inverters, Converters, Controllers and Interconnection System Equipment for Use with Distributed Energy Resources. Underwriters Laboratories: Northbrook, IL, USA, 2010.
41. *CSA C22.2 No. 14*; Industrial Control Equipment. Canadian Standards Association: Toronto, ON, Canada, 2018.
42. *CSA C22.2 No. 107.1*; General Use Power Supplies. Canadian Standards Association: Toronto, ON, Canada, 2018.
43. *CSA C22.2 No. 286*; Standard for Adjustable Speed Drives. Canadian Standards Association: Toronto, ON, Canada, 2010.
44. Canadian Standards Association. Available online: https://www.csagroup.org/standards/standards-research/ (accessed on 11 January 2026).
45. American Bureau of Shipping. Available online: https://ww2.eagle.org/en/rules-and-resources/rules-and-guides/archives.html (accessed on 11 January 2026).
46. International Organization for Standardization. Standards. Available online: https://www.iso.org/standards.html (accessed on 11 January 2026).
47. *ISO 9001*; Quality Management Systems—Requirements. International Organization for Standardization: Geneva, Switzerland, 2015.
48. Davoodi, M.; Bevrani, H. A new application of the hardware in the loop test of the min–max controller for turbofan engine fuel control. *Adv. Control Appl. Eng. Ind. Syst.* **2023**, *5*, e138. [CrossRef]
49. Mirus International Inc. Available online: https://www.mirusinternational.com/ (accessed on 11 January 2026).